



**GEOLOGICAL SURVEY OF CANADA
OPEN FILE 7853**

**Targeted Geoscience Initiative 4: Contributions to the
Understanding of Volcanogenic Massive Sulphide Deposit
Genesis and Exploration Methods Development**

**Multiple sulphur isotope reconnaissance of Slave Province volcanogenic massive
sulphide deposits**

Bruce E. Taylor¹, Jan M. Peter¹, and Boswell A. Wing²

¹Geological Survey of Canada, Ottawa, Ontario

²McGill University, Montreal, Quebec

2015

© Her Majesty the Queen in Right of Canada, as represented by the Minister of Natural Resources Canada, 2015

This publication is available for free download through GEOSCAN (<http://geoscan.nrcan.gc.ca/>)

Recommended citation

Taylor, B.E., Peter, J.M., and Wing, B.A., 2015. Multiple sulphur isotope reconnaissance of Slave Province volcanogenic massive sulphide deposits, *In: Targeted Geoscience Initiative 4: Contributions to the Understanding of Volcanogenic Massive Sulphide Deposit Genesis and Exploration Methods Development*, (ed.) J.M. Peter and P. Mercier-Langevin; Geological Survey of Canada, Open File 7853, p. 45–58.

Publications in this series have not been edited; they are released as submitted by the author.

Contribution to the Geological Survey of Canada's Targeted Geoscience Initiative 4 (TGI-4) Program (2010–2015)

TABLE OF CONTENTS

Abstract	47
Introduction	47
Background	47
Sample Selection and Methodology	49
Results	51
Discussion	51
Evidence and Assessment of Mass-Independent Fractionation in Slave Volcanogenic Massive Sulphide Deposits	53
Sulphur Sources in Archean Volcanogenic Massive Sulphide Deposits of the Slave Province	54
Slave Province-Wide Variations in $\delta^{34}\text{S}$ and $\Delta^{33}\text{S}$	54
Relationships between $\delta^{34}\text{S}$ and $\Delta^{33}\text{S}$, Tectonic Setting, and Silver Contents in Selected Volcanogenic Massive Sulphide Deposits in the Slave Province	54
Implications for Exploration	56
Summary and Conclusions	56
Future Work	57
Acknowledgements	57
References	57
Figures	
Figure 1. Generalized geological map of the Slave Craton showing the locations of volcanogenic massive sulphide deposits included in this study	48
Figure 2. Plot of $\delta^{33}\text{S}$ vs. $\delta^{34}\text{S}$ illustrating the mass-dependent fractionation that has dominated S-isotope abundances since ca. 2.0 Ga	49
Figure 3. Schematic diagram of an Archean volcanogenic massive sulphide-producing submarine hydrothermal system illustrating sources, sinks, and general fractionation tendencies for sulphur isotopes in two principal tectonic settings	49
Figure 4. Plot of $\Delta^{33}\text{S}$ versus age for sulphides illustrating the presence of marked mass-independent fractionation in the isotopic record prior to ca. 2.45 Ga	50
Figure 5. Schematic diagram of the Micro-Isotopic Laser Extraction System plus Stanford Research Institute gas chromatograph	51
Figure 6. Histograms of $\delta^{34}\text{S}$ and $\Delta^{33}\text{S}$ values of pure and mixed sulphide from volcanogenic massive sulphide deposits in the Slave Province	52
Figure 7. Plot of $\delta^{34}\text{S}$ versus age for both sulphides and sulphates	52
Figure 8. Plot of $\delta^{33}\text{S}$ versus $\delta^{34}\text{S}$ for pure pyrite, galena, sphalerite, or mixtures dominated by one of these minerals	53
Figure 9. Plot of $\Delta^{33}\text{S}$ versus $\delta^{34}\text{S}$ for pure and mixed sulphides from Slave Province volcanogenic massive sulphide deposits analyzed in this study	53
Figure 10. Map showing the distribution and, in some cases, range, of $\delta^{34}\text{S}$ values for pure and mixed sulphide samples from volcanogenic massive sulphide deposits in the Slave Craton	55
Figure 11. Map showing the distribution and range of $\Delta^{33}\text{S}$ for pure and mixed sulphide samples from volcanogenic massive sulphide deposits in the Slave Craton	55
Figure 12. Comparison of $\Delta^{33}\text{S}$ values from selected volcanogenic massive sulphide deposits, grouped according to their interpreted tectonic environment	56

Multiple sulphur isotope reconnaissance of Slave Province volcanogenic massive sulphide deposits

Bruce E. Taylor^{1*}, Jan M. Peter¹, and Boswell A. Wing²

¹Central Canada Division, Geological Survey of Canada, 601 Booth Street, Ottawa, Ontario K1A 0E8

²Department of Earth and Planetary Sciences, McGill University, 3450 University Street, Montreal, Quebec H3A 2A7

*Corresponding author's e-mail: btaylor@nrcan-rncan.gc.ca

ABSTRACT

Multi-sulphur isotope (³²S, ³³S, ³⁴S, and ³⁶S) analysis of galena, sphalerite, and pyrite from 30 Archean volcanogenic massive sulphide deposits and occurrences from across the Slave Province reveals a variable contribution from Archean atmosphere-derived sulphur. Mass-independent fractionation of the sulphur isotopes produced anomalous abundances ($\Delta^{33}\text{S}$) of the sulphur isotopes that were incorporated to varying degrees in deposits that formed in different tectonic settings. Our data indicate that deposits of the bimodal-mafic type (bimodal rift setting) are characterized by a restricted range of $\Delta^{33}\text{S}$ from -0.3 to 0.1 per mil, whereas deposits of the bimodal-felsic type (arc-like settings) exhibit a broader range in $\Delta^{33}\text{S}$, from -0.8 to 0.6 per mil. Mantle-derived (juvenile) sulphur is essentially the sole source of sulphur in deposits of the bimodal-mafic type, whether derived directly by magmatic degassing, or indirectly by leaching of magmatic sulphides in the associated hydrothermal system; these deposits are also characterized by relatively low silver contents. Bimodal-felsic type deposits, typified by high silver contents, contain variable amounts of atmosphere-derived sulphur that was more readily available in arc-like settings.

INTRODUCTION

Herein we present the results of a reconnaissance study of the multiple sulphur isotope compositions of sulphides from 30 selected Archean volcanogenic massive sulphide (VMS) deposits or occurrences in the Slave Province (Fig. 1). Several of these VMS deposits (notably High Lake, Hackett River, and Izok Lake) have significant contents of precious metals, in particular Ag. Bleeker and Hall (2007 and references therein) described two major subdivisions of volcanism in the Slave Province: mafic, rift-related volcanism (ca. 2.73–2.70 Ga and 2.70–2.66 Ga) and transitional to calc-alkaline arc-like volcanism. Both occurred on an ancient basement complex, with crustal ages becoming younger to the east (Bleeker and Hall, 2007). These volcanic rocks were deposited in two different tectonic environmental settings, with the older (ca. 2.73–2.70 Ga) rocks in bi-modal rift settings, and the younger (post-2.70 Ga) rocks in arc-like settings, in which calc-alkaline volcanism occurred. VMS deposits occur in rocks of both these time periods. We conducted a reconnaissance multiple sulphur isotope investigation of sulphide minerals from VMS deposits throughout the Slave Province. In rocks older than ca. 2.2 Ga, and especially those older than 2.45 Ga, mass-independent fractionation (MIF) of sulphur provides a unique environmental tracer. Our goals were to ascertain whether

the sulphur isotope compositions reflect these different ages of volcanism, and host-rock lithogeochemical and deposit metal contents.

BACKGROUND

Prior to ca. 2.45 Ga, the distribution of sulphur isotopes was characterized by production of anomalous amounts of ³³S through photolysis reactions in the atmosphere involving volcanic SO-SO₂ (Farquhar et al., 2000, 2001). The result of this process, which was able to proceed due to the absence of an ozone layer and to low pressures (concentrations) of atmospheric oxygen, was the mass-independent fractionation (MIF) of the isotopes of sulphur and the creation of a unique tracer of surface-processed sulphur (e.g. Farquhar and Wing, 2003). A brief discussion of the causes and effects of MIF follows in order to provide background for discussion of the data acquired in this study.

The typical mass-dependent fractionation (MDF) relationship between ³³S and ³⁴S is shown by the linear trend of values in Figure 2 and is contrasted with the trend for MIF, which is indicated by positive and negative values of $\Delta^{33}\text{S}$ ($= \delta^{33}\text{S}_{\text{MEASURED}} - \delta^{33}\text{S}_{\text{MDF-PREDICTED}}$; see Fig. 2), relative to MDF, which is defined by the equation $\delta^{33}\text{S} = 0.515 \delta^{34}\text{S}$ (Farquhar et al., 2000). In the absence of the shielding effects of ozone during the Archean, MIF is thought to have been

Taylor, B.E., Peter, J.M., and Wing, B.A., 2015. Multiple sulphur isotope reconnaissance of Slave Province volcanogenic massive sulphide deposits, *In*: Targeted Geoscience Initiative 4: Contributions to the Understanding of Volcanogenic Massive Sulphide Deposit Genesis and Exploration Methods Development, (ed.) J.M. Peter and P. Mercier-Langevin; Geological Survey of Canada, Open File 7853, p. 45–58.

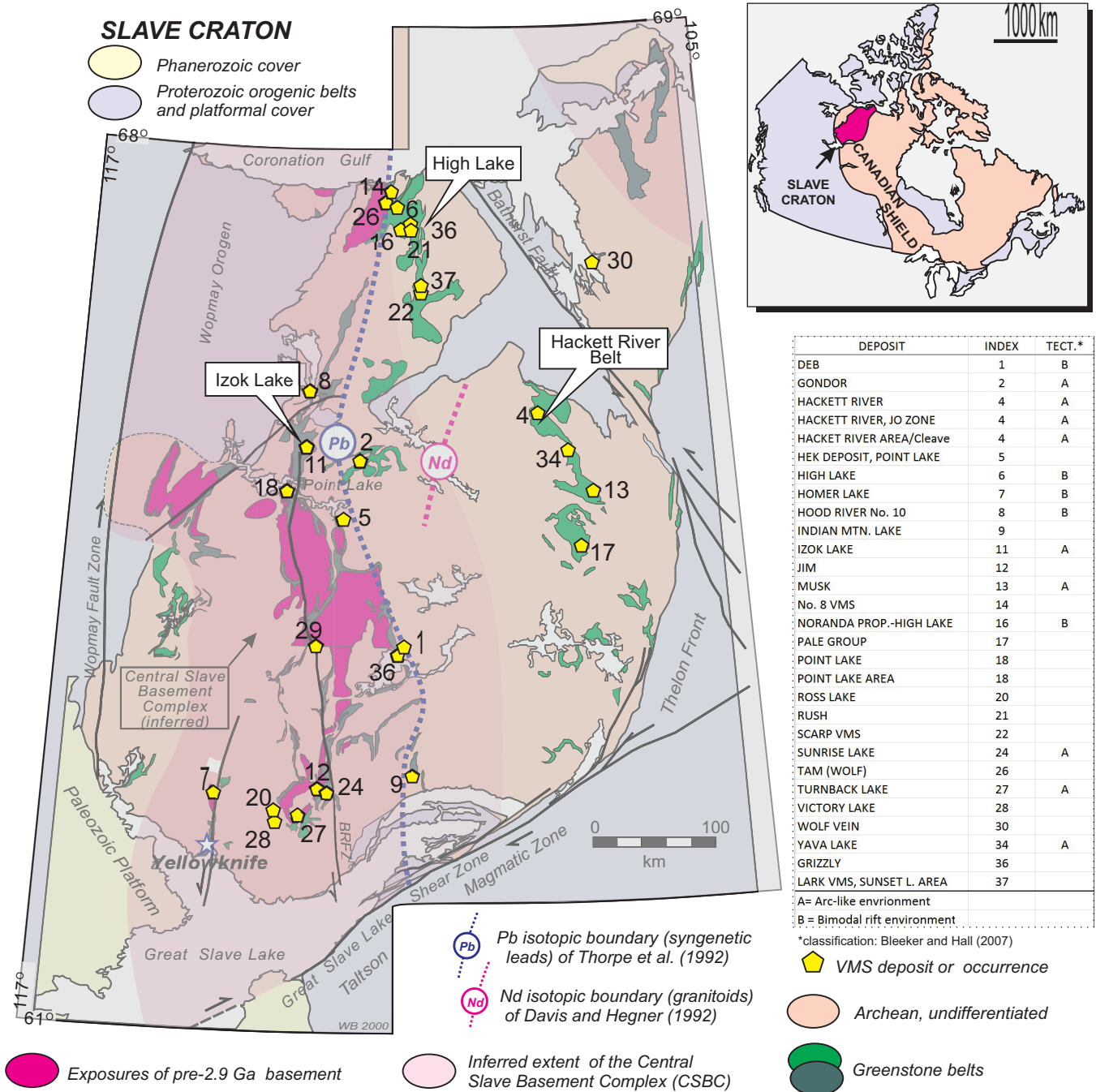


Figure 1. Generalized geological map of the Slave Craton (Province) (after Bleeker and Hall, 2007), showing the locations of volcanogenic massive sulphide deposits included in this study (see index for deposit names, numbers, and tectonic environments). Undifferentiated Archean rocks include granitoid, gneiss, and turbidite sequences. Tholeiitic greenstone belts are indicated by the darker green colour. Exposures of pre-2.9 Ga basement, and boundaries based on Pb isotopes in deposits (Thorpe et al., 1992) and on Nd isotopes in granitoid rocks (Davis and Hegner, 1992) are shown for reference.

caused by UV photolysis of atmospheric SO₂-SO, resulting in an excess or depletion of ³³S relative to that produced by mass-dependent fractionation of sulphur among existing sulphur-bearing compounds (Farquhar et al., 2000). The resulting MIF sulphur is transported to the Earth's surface as native sulphur (S⁰; Δ³³S > 0) or sulphate (H₂SO₄; Δ³³S < 0), and incorporated in pyrite via bacterial (BSR) or thermal (TSR) sulphate

reduction. These processes are schematically shown in the context of a seafloor hydrothermal system in Figure 3. MIF was a significant process prior to 2.45 Ga. Thus, non-zero Δ³³S values are a unique, chemically conservative tracer/signal of atmospheric sulphur that can be variably present in pre-2.45 Ga paleohydrothermal systems. This MIF signal cannot be modified or masked by MDF processes, but is susceptible to dilution.

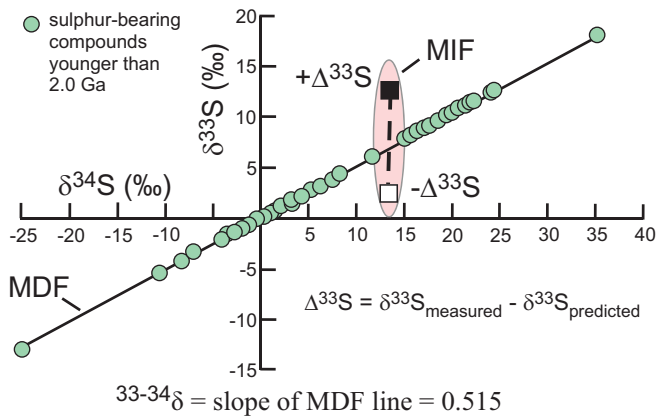


Figure 2. Plot of $\delta^{33}\text{S}$ versus $\delta^{34}\text{S}$ illustrating the mass-dependent fractionation (MDF; $\delta^{33}\text{S} = 0.515 \delta^{34}\text{S}$) that has dominated S-isotope abundances since ca. 2.0 Ga (modified from Farquhar et al., 2001; Farquhar and Wing, 2003). Prior to that, an atmosphere depleted in ozone and oxygen facilitated photochemical fractionation of ^{33}S relative to ^{34}S from atmospheric $\text{SO}-\text{SO}_2$, resulting in mass-independent fractionation (MIF) of the sulphur isotopes ($\Delta^{33}\text{S}$), with reduced sulphur products enriched in ^{33}S (verified) and oxidized sulphur products depleted in ^{33}S sulphates (predicted, but not yet corroborated).

Archean oceans are generally thought to have been low in sulphate, with $\Delta^{33}\text{S} \approx 0$ (e.g. Jamieson et al., 2013), but details remain controversial.

The occurrence of the MIF signal in sulphides as a function of geological age is shown in Figure 4, where the abrupt presence of a marked MIF signal at ca. 2.45 Ga, and older, is apparent. The apparently sudden onset of a MIF signal (Fig. 4) has been attributed to a rapid oxygenation of the Earth’s atmosphere and termed the “Great Oxidation Event” (GOE) (e.g. Holland, 2006). Although the onset of a MIF signal appears abrupt in this figure, the oxidation of the Earth’s atmosphere was not sudden and linear, but gradual and punctuated (e.g. Ohmoto, et al., 2006; Pufahl and Hiatt, 2012; Planavsky et al, 2014). Since 2.0 Ga, however, sulphur isotope distribution has been controlled by the MDF processes, which have dominated over MIF processes.

SAMPLE SELECTION AND METHODOLOGY

Sulphide samples were selected from the archived collection of Ralph Thorpe (formerly, Geological Survey

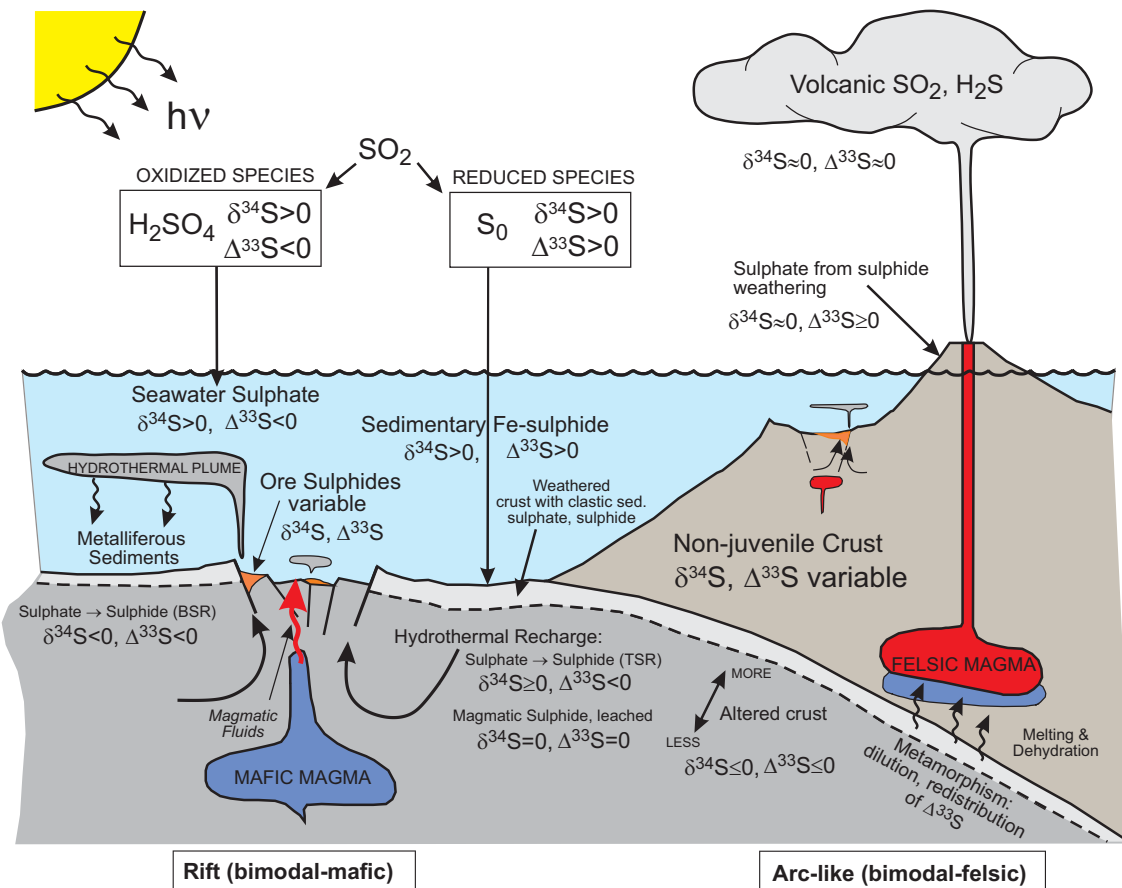


Figure 3. Schematic diagram of an Archean volcanogenic massive sulphide-producing submarine hydrothermal system illustrating sources, sinks, and general fractionation tendencies for sulphur isotopes in two principal tectonic settings (adapted, in part, from Farquhar and Wing, 2003 and Sharman et al., in press). The mass-independent fractionation (MIF) “signal” (i.e., $\Delta^{33}\text{S} \neq 0$) is thought to derive from photolysis reactions involving atmospheric (volcanic) SO_2 . Microbial sulphate reduction (BSR) and hydrothermal sulphate reduction (TSR) forms sulphides with $\Delta^{33}\text{S} < 0$. Such sulphate-reduction systems were generally similar to those operating today. Mixing of sulphur sources may dilute the MIF signal in some crustal sinks.

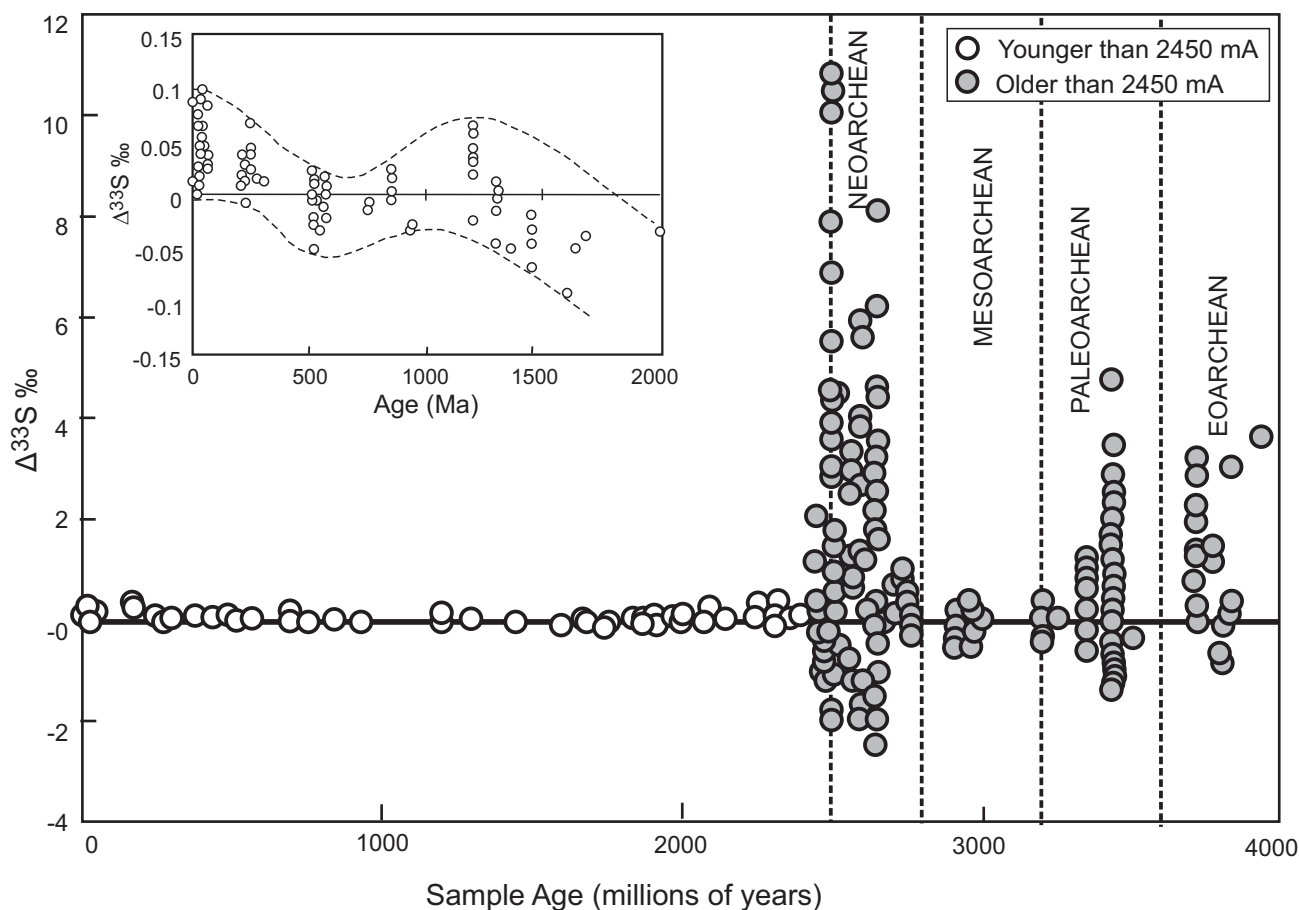


Figure 4. Plot of $\Delta^{33}\text{S}$ versus age for sulphides (from Farquhar et al., 2010) illustrates the presence of marked mass-independent fractionation (MIF) in the isotopic record prior to ca. 2.45 Ga. A subsequent, rapid increase in atmospheric oxygen is inferred to have occurred about 2.45 Ga, after which MDF dominated. Inset illustrates minor ($\pm 0.1\%$) variation in $\Delta^{33}\text{S}$ of marine sulphate since about 2.0 Ga.

of Canada) for Pb isotope analysis (see Thorpe, 2008) with the aim to select as geographically representative a set of samples as possible. In some cases the samples analyzed in this study were aliquots of the same galena concentrates previously analyzed for lead isotopes (Thorpe et al., 2008). In numerous cases, however, hand-picked separates of pure pyrite, sphalerite, or galena prepared from small chip samples of massive sulphide were used. In a few instances, the small grain size precluded efficient purification to 100%, and the analyzed samples also contained small amounts of silicate minerals and/or other sulphides.

Sulphide samples of 1 to 3 mg size were converted to SF_6 (generally $<5 \mu\text{mol}$ total yield) by laser-assisted fluorination in an atmosphere of 100% pure F_2 using a micro-isotopic laser extraction system (MILES; Taylor, 2004), modified by the addition of a Stanford Research Institute[®] gas chromatograph (model 310), dedicated computer and control software, and associated high-vacuum line with gas chromatograph- (GC) multiport valves for injecting/collecting sample splits (Fig. 5). The SF_6 generated by the fluorination reaction was cryogenically separated from non-condensable by-

product gases and excess F_2 at -192°C and then passed through a variable temperature trap at -135°C for additional purification before further on-line purification over two GC columns in series: Haysep Q (2 m length) and Molsieve 5A (2 m length) at 60°C by means of a pure He carrier gas at a rate of 25 mL/min. The SF_6 was isolated from contaminants and the carrier gas by means of a high-efficiency cold finger at -192°C (Taylor, 2004) and sealed in 6 mm glass tubes for subsequent analysis by mass spectrometry. The sealed gases were analyzed for the four stable isotopes of sulphur (^{32}S , ^{33}S , ^{34}S , ^{36}S) in a Thermo-Electron MAT 253 isotope ratio mass spectrometer in the Department of Earth and Planetary Sciences, McGill University, Montreal. The mass spectrometer was fitted with a dual inlet, micro-volume and a custom-built (B.E. Taylor) inlet manifold designed for use with micro samples.

Results are reported using the standard δ -notation, in per mil (‰) relative to V-CDT. Uncertainties in $\delta^{34}\text{S}$, as determined on duplicates, were typically $<0.2\%$ and $<0.02\%$ for $\Delta^{33}\text{S}$. However, the technical challenges of irregular intervals between sample extraction (Ottawa) and mass spectrometry (Montreal), may have added

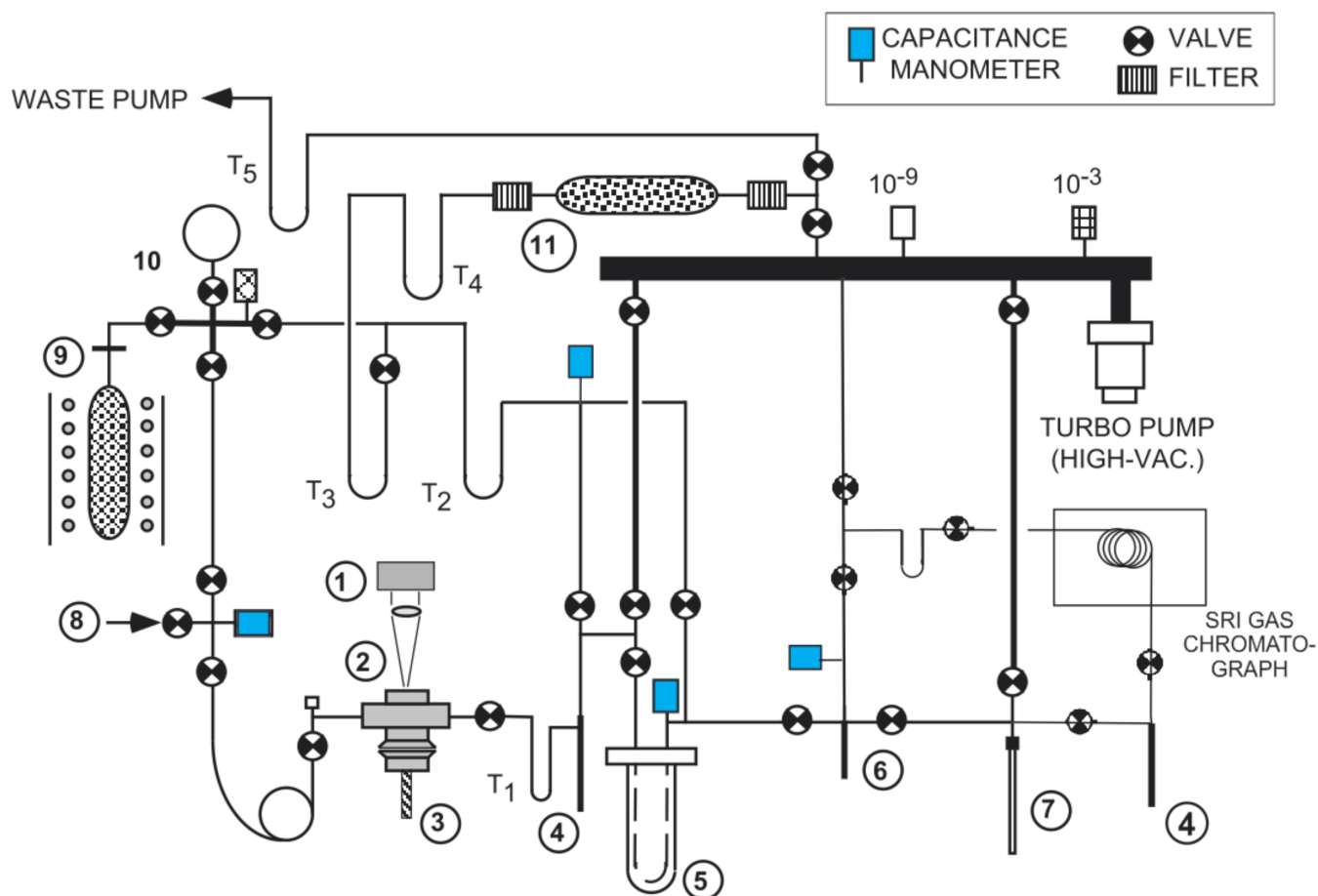


Figure 5. Schematic diagram of MILES+GC (Micro-Isotopic Laser Extraction System) plus Stanford Research Institute® gas chromatograph (Model 310). Components include (1) zoom stereo microscope; (2) Synrad® 25 watt CO₂ laser and beam delivery system; (3) small-volume sample chamber, with individual Ni crucibles (for grains), or flat stage (for in situ analysis), and cooling finger; (4) fritted P-trap (100% efficient separation of condensable sample from carrier gas); (5) variable temperature trap for cryogenic separations; (6) mini P-trap/manometer; and (7) 6 mm cracker tube (Pyrex® glass) for collection of purified SF₆ sample. Associated GC valves and high-vacuum piping for sample injection onto GC columns (see text) not illustrated for simplicity (modified from Taylor, 2004).

slightly to the external uncertainty of each analysis due to the necessity of using multiple small aliquots of reference gas. Some gas chromatographic spectra of product gases from fluorination of sulphide samples containing trace to minor amounts of silicates yielded peaks of another gas (likely SOF₂) in addition to SF₆. Although this appears to have had little effect on the $\delta^{34}\text{S}$ values in sulphide-silicate mixtures up to 1:1 (B.E. Taylor, unpub.), potential effects on other isotopes are unknown.

RESULTS

Figure 6a plots the 72 $\delta^{34}\text{S}$ values (‰, V-CDT) of pure and mixed sulphides (i.e. concentrates of pyrite, sphalerite, and/or galena, with traces of other sulphides or silicates in a few samples) from VMS deposits in the Slave Province obtained in this study that exhibit a distribution of approximately -2 / $+4$ ‰ about a mean $\delta^{34}\text{S}$ value of 0.77‰; range: -2.5 to 3.9‰, with two outliers. The mean value and small range of $\delta^{34}\text{S}$ values are

indicative of mantle-dominated Archean sulphur. The distribution of $\Delta^{33}\text{S}$ values for pure and mixed sulphides (defined as in Fig. 6a) from Slave Province VMS deposits shown in Figure 6b indicates a slight predominance of negative $\Delta^{33}\text{S}$ values (mean value = -0.08 ‰; range: -1.03 to 1.53‰) that indicates the involvement of sulphur generated by MIF processes.

DISCUSSION

The incorporation of ³³S in abundances that deviate from those determined by mass-dependent fractionation (i.e. $\delta^{33}\text{S} = 0.515 \delta^{34}\text{S}$) in sulphides from Archean VMS deposits signifies that mass-independent fraction (MIF) signatures resulting from photolysis of atmospheric SO₂ are preserved in hydrothermal systems (Farquhar and Wing, 2003). The deviation from the MDF equation for sulphur isotopes (Fig. 2) provides a unique tracer of the involvement of surface processed (atmospheric-derived) sulphur in VMS deposits older than 2.45 Ga (e.g. Farquhar et al., 2010).

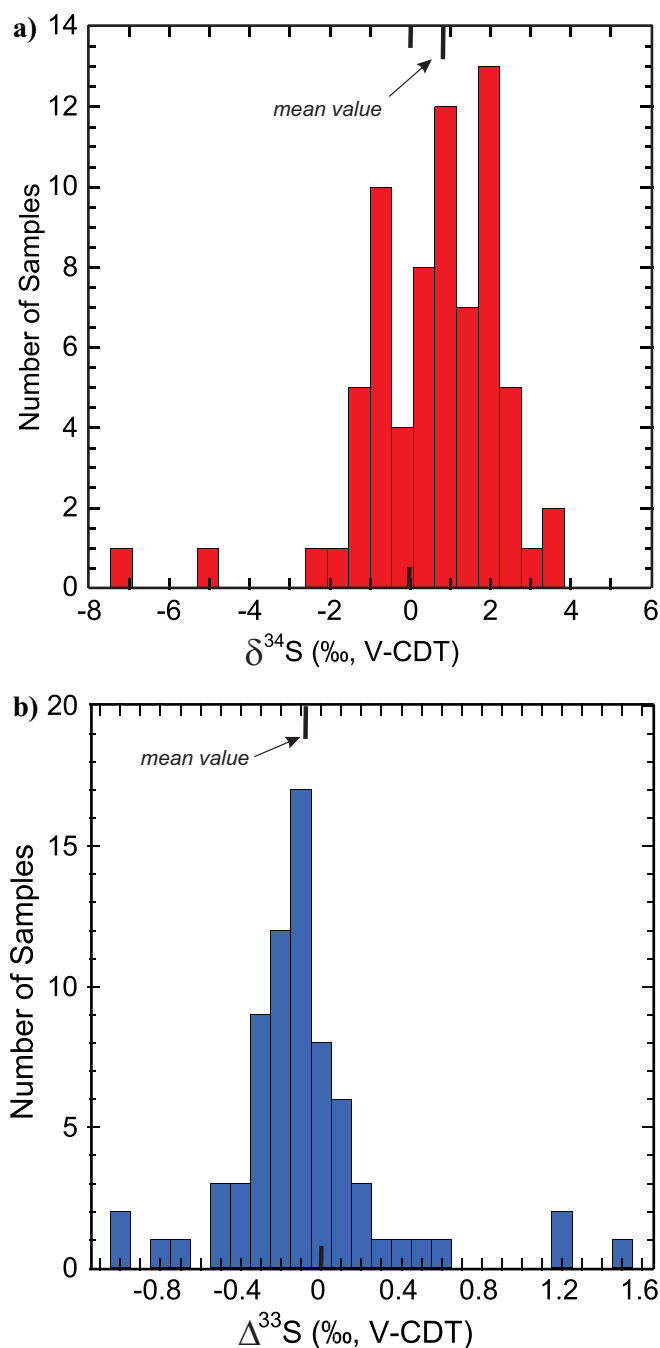


Figure 6. **a)** Histogram of $\delta^{34}\text{S}$ values (‰, V-CDT; $n=72$) of pure and mixed sulphide (a concentrate of pyrite, sphalerite, and/or galena; traces of other sulphides, or silicate possible in some samples) from volcanogenic massive sulphide (VMS) deposits in the Slave Province (this study). The mean $\delta^{34}\text{S}$ value (0.77‰) and range of $\delta^{34}\text{S}$ values are indicative of a dominance of mantle-dominated Archean sulphur. **b)** Histogram of $\Delta^{33}\text{S}$ values (‰, V-CDT; $n=72$) of pure and mixed sulphide samples (as in Fig. 6a) from Slave Province VMS deposits depicts a normal distribution with a mean value of -0.08‰, and a range typical of rocks older than ca. 2.45 Ga (e.g. ± 1.0 ‰). Although the primitive mantle value ($\Delta^{33}\text{S} = 0$) dominates, incorporation of surface-derived sulphur (indicated by $\Delta^{33}\text{S} \neq 0$) is apparent in a significant number of the samples.

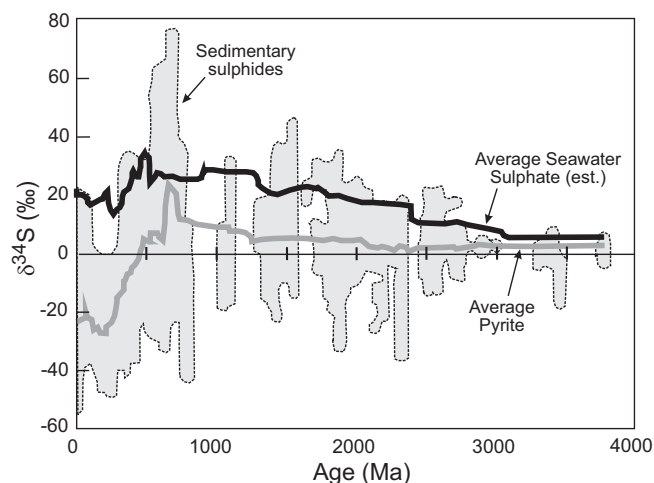


Figure 7. Plot of $\delta^{34}\text{S}$ versus age for both sulphides and sulphates. A running average composition of sulphide is shown by the gray curve, and for that of sulphate by the black curve (modified after Farquhar et al, 2010).

Archean seawater sulphate is thought to be characterized by rather homogeneous, negative values of $\Delta^{33}\text{S}$ (approximately -2‰; Zhelezinskaia et al., 2014), due to the low sulphate contents of Archean seawater, limited BSR, and mass balance considerations upon SO_2 photolysis (Farquhar et al., 2000; Fig. 7). However, recent investigations of trace sulphate contained in marine carbonate (so-called carbonate-associated sulphate; CAS), have reported positive values of $\Delta^{33}\text{S}$ up to ~ 10 ‰ (Paris et al., 2014). Moreover, the apparent absence of large sulphur-isotope fractionations between sulphide and sulphate in Archean rocks has been accepted as an indication of limited microbial sulphate reduction (Zhelezinskaia et al., 2014).

Zhelezinskaia et al. (2014) report large negative values of $\delta^{34}\text{S}$ to approximately -40‰, with uniform negative values of $\Delta^{33}\text{S}$ in one carbonate unit, determined using secondary ion mass spectrometry (SIMS) that indicates marked bacterial sulphate reduction (BSR), despite very low aqueous sulphate levels. However, neither SO_2 - nor SF_6 -based techniques have yielded such negative $\delta^{34}\text{S}$ values for these same samples (lower limit of approximately -17‰), and this implies that there is high isotopic variability at the microscopic scale; SIMS and SF_6 -based analyses are in good agreement for $\Delta^{33}\text{S}$ (Zhelezinskaia et al., 2014). The implications of this new finding are not yet fully understood. Although the incorporation in Archean sulphides of ^{33}S by MIF provides a clear atmospheric signal, the Archean sulphur cycle remains incompletely understood, including the preservation of an atmospheric $\Delta^{33}\text{S}$ signal during subsequent MDF processes.

All of the VMS deposits in the Slave Province sampled for this study (Fig. 1) satisfy the age criterion for

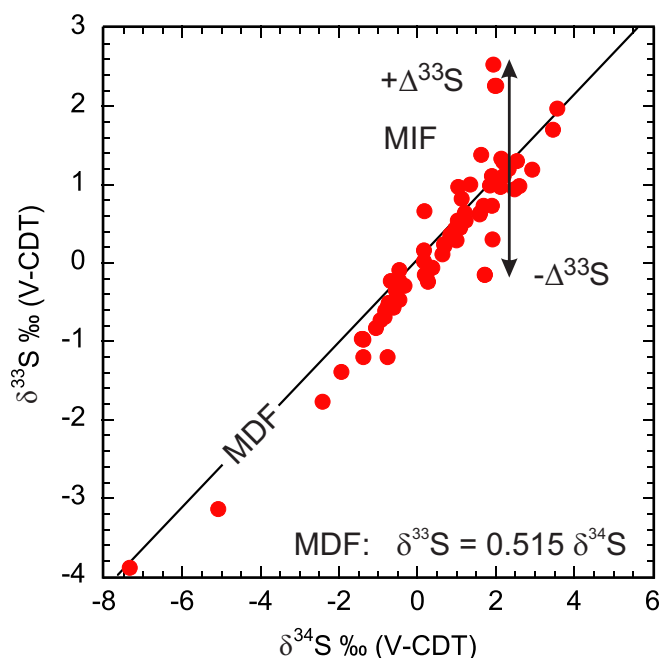


Figure 8. Plot of $\delta^{33}\text{S}$ versus $\delta^{34}\text{S}$ for pure pyrite, galena, sphalerite, or mixtures dominated by one of these minerals. Line for mass-dependent fractionation (MDF; $\Delta^{33}\text{S} = 0.515 \delta^{34}\text{S}$) is shown for reference. Deviation from the MDF trend due to mass-independent fractionation (MIF) indicates variable, significant contributions of surficial (surface-processed) sulphur. Symbol size is approximately ten times larger than the uncertainty.

effective use of $\Delta^{33}\text{S}$ to detect surficially processed sulphur. Our intent was to document any differences in $\delta^{34}\text{S}$ and $\Delta^{33}\text{S}$ among the deposits sampled, and if present, determine whether they correlate with isotopic markers of crustal age and provenance: Nd isotope line of Davis and Hegner (1992); Pb isotope line of Thorpe et al. (1992) (see Fig. 1). In addition, we investigated whether our data would have implications for the origin of VMS deposits in the Slave Province with regard to either their tectonic environments or their Ag contents.

Evidence and Assessment of Mass-Independent Fractionation in Slave Volcanogenic Massive Sulphide Deposits

Deviation of isotopic compositions from the MDF relationship ($\delta^{33}\text{S} = 0.515 \delta^{34}\text{S}$) provides the criterion for MIF (see Fig. 8). Samples cover a broad range of $\delta^{33}\text{S}$ and $\delta^{34}\text{S}$, and some correspond to the above equation. However, both positive and negative deviations from the MDF equation, indicated by $+\Delta^{33}\text{S}$ and by $-\Delta^{33}\text{S}$, respectively, shown in Figure 8, demonstrate the clear presence of MIF in many samples. Zhelezinskaia et al. (2014) suggest that VMS deposits with $-\Delta^{33}\text{S}$ are likely an important sink for atmospheric sulphate.

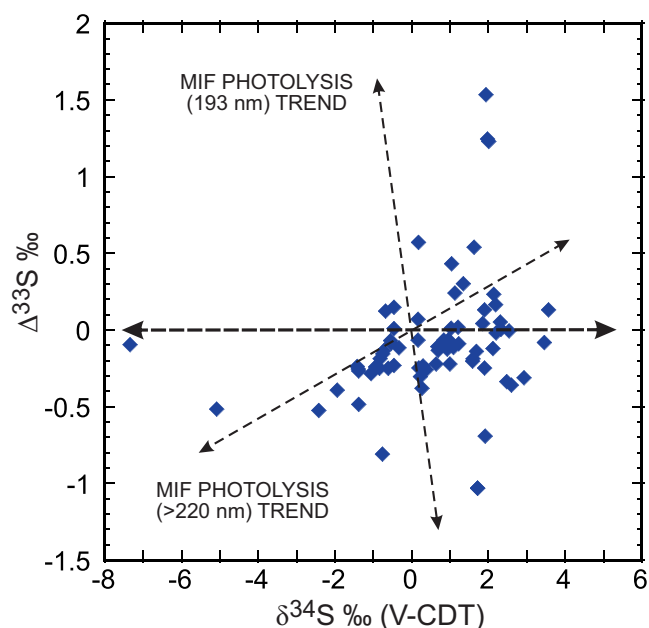


Figure 9. Plot of $\Delta^{33}\text{S}$ vs $\delta^{34}\text{S}$ for pure and mixed sulphides from Slave Province volcanogenic massive sulphide deposits analyzed in this study; the data indicate marked mass-independent fractionation (MIF), and mimic trends of experimental arrays based on photolysis experiments (after Farquhar and Wing, 2003). MIF trends for photolysis reactions in experiments using 193 nm wavelength and >220 nm wavelength light sources under low pressures of CO and O; other arrays are discussed in the text. The correspondence between the arrays and the Slave Province results is consistent with photolysis of Archean atmospheric SO_2 to explain the marked MIF.

Complete thermal sulphate reduction (TSR) of dissolved marine sulphate with a $-\Delta^{33}\text{S}$ signature in the flow paths of circulating hydrothermal seawater fluids (Fig. 3) would result in reduced sulphur with negative $\Delta^{33}\text{S}$ values. When combined with magmatic sulphur (leached and/or degassed), the resulting VMS sulphides would have values of $\Delta^{33}\text{S} \leq 0$. Our data for sulphides from Slave VMS deposits (Fig. 8) are consistent with such a scenario for most samples. Galena from the Jo Zone at Hackett River is the most negative $\Delta^{33}\text{S}$ value (-0.810 ‰) recorded in our study.

Details regarding the origin of MIF of sulphur isotopes are still a matter of some debate. Photolysis experiments on SO_2 using ultraviolet light, particularly the 193 nm wavelength (Farquhar et al., 2001), demonstrate striking MIF effects, although other wavelengths may also be important (Farquhar and Wing, 2003; Paris et al., 2014). Reaction products include S^0 with lower $\delta^{34}\text{S}$ and higher $\Delta^{33}\text{S}$ than the initial SO_2 ; residual SO_2 and product sulphate have higher values of $\delta^{34}\text{S}$ and lower values of $\Delta^{33}\text{S}$. Comparison of $\Delta^{33}\text{S}$ and $\delta^{34}\text{S}$ for Slave Province VMS sulphides with experimentally determined fractionation trends for photolysis-induced MIF suggests a general agreement with a UV-photolysis origin (Fig. 9).

Sulphur Sources in Archean Volcanogenic Massive Sulphide Deposits of the Slave Province

The similarity in the topologies of the curves for the mean $\delta^{34}\text{S}$ values of sulphides in VMS deposits and marine sulphate versus age has influenced the variation (from greatest to least) inferred for role of seawater sulphate in VMS deposits in three different hypotheses: (1) incorporation by bacterial sulphate reduction by BSR (Sangster, 1968); (2) partial reduction of seawater sulphate by TSR, plus leaching of wall-rock sulphide (Sasaki, 1970); and (3) partial reduction of sulphate to sulphide, plus leaching of wall-rock sulphide during water/rock interaction in the “anhydrite buffer model” (Ohmoto et al., 1983). In the Archean, MIF sulphur isotope abundances in VMS deposits (i.e. $\Delta^{33}\text{S} \neq 0$) similarly provide seemingly incontrovertible evidence for incorporation of some surficial sulphur, despite estimates of the low concentration of sulphate in seawater (e.g. <80 ppm, or $\mu\text{mol/litre}$: Jamieson et al., 2013; <1000 ppm: Zhelezinskaia et al., 2014). Estimates of the amount of seawater sulphate incorporated in Archean VMS based on $\Delta^{33}\text{S}$ are low ($\leq 3\%$: Jamieson et al., 2013; $\leq 25\%$: Sharman et al., in press; see also Ono et al., 2007), despite the assertion of Zhelezinskaia et al. (2014) that VMS deposits should constitute a significant sink for atmospheric sulphate.

Jamieson et al. (2013) document a maximum of 3% seawater sulphate in the giant Neoproterozoic Kidd Creek deposit based on multi-sulphur isotope data. Detailed multi-sulphur isotope analyses of VMS deposits in the ca. 2.7 Ga Noranda complex (Abitibi subprovince) by Sharman et al. (in press) concluded that both magmatic sulphur (directly contributed or leached) and surface-processed sulphur were incorporated in the sulphide mineralization. Magmatic sulphur is interpreted to have been the dominant sulphur source for the central Noranda camp VMS deposits, with the contribution of surficial sulphur increasing during evolution of the Noranda caldera. Deposits formed on the margin of the caldera contain $<5\%$ sulphur originating from seawater sulphate, whereas sulphide deposits that formed later in the caldera’s evolution contain up to 25% (Sharman et al., in press). For comparison, Ono et al. (2007) used high-precision multi-sulphur isotope analysis to conclude that seawater sulphate contributes 11 to 27% of the sulphur comprising vent sulphides in the modern day TAG (Trans-Atlantic Geotraverse) hydrothermal field. The maximum estimated present-day seawater sulphate contribution (27%; Ono et al., 2007) is in good agreement with the maximum contribution ($\leq 25\%$) estimated for VMS deposits in the Noranda caldera by Sharman et al. (in press), and consistent with the estimate of Jamieson et al. (2013) for the Archean Kidd Creek deposit. From this we infer that

the dominant source of sulphur in the Slave Province VMS deposits is of magmatic (mantle) origin (i.e. $\delta^{34}\text{S} \approx 0$; $\Delta^{33}\text{S} \approx 0$). Although consistent with a direct magmatic origin (i.e. by magmatic degassing), Ono et al. (2007) demonstrated that 73 to 89% of the sulphur in the modern seafloor VMS system at TAG was derived by leaching from the underlying basalt during hydrothermal alteration. Derivation of all or the majority of sulphur in VMS from reduction of seawater sulphate is, thus, not required. Contributions of ~ 10 to 30% sulphur derived from seawater sulphate to VMS are sufficient to explain the topological similarity of the age versus $\delta^{34}\text{S}$ curves for both sulphur in VMS deposits (see Huston, 1999 and references therein) and seawater sulphate (Claypool, et al., 1980). Below, we consider the implications of variation in the contribution of seawater sulphate to Slave VMS deposits for their environment of formation.

Slave Province-Wide Variations in $\delta^{34}\text{S}$ and $\Delta^{33}\text{S}$

The values of $\delta^{34}\text{S}$ determined for VMS samples from the Slave Province are plotted on a geological base map of the province in Figure 10, which shows the age of basement rocks, geographic locations of greenstone belts, and, for reference, Pb- and Nd-isotope divisions/boundaries of the Slave crust. No correlations with any of these features are apparent. Figure 11 plots the $\Delta^{33}\text{S}$ ranges for sulphides from VMS deposits across the Slave Province on the same geological base map as in Figure 10. At the province-wide scale, there are no correlations apparent with the same features outlined above; however, any correlations would be complicated by the relatively narrow range of $\Delta^{33}\text{S}$ involved, the reconnaissance nature (possible non-representativeness) of our database, the relatively limited number of samples from each sample site, and the comparison of sulphide concentrates with pure minerals.

The lack of correlations of the ranges of $\delta^{34}\text{S}$ and $\Delta^{33}\text{S}$ with geographic location or geology indicates that processes and sulphur sources were similar in the formation of all of the Slave VMS deposits.

Relationships between $\delta^{34}\text{S}$ and $\Delta^{33}\text{S}$, Tectonic Setting, and Silver Contents in Selected Volcanogenic Massive Sulphide Deposits in the Slave Province

Two different tectonic settings were suggested by Bleeker and Hall (2007) for several of the VMS deposits analyzed in this study: an arc-like environment and a bimodal-rift environment (see Figs. 1 and 3). The tectonic styles and settings of Archean greenstone belts in general (and the VMS-hosting Slave greenstone belts specifically) remains a matter of some debate and uncertainty (e.g. Cawood et al., 2006). For most of the deposits discussed below and shown in

Multiple sulphur isotope reconnaissance of Slave Province volcanogenic massive sulphide deposits

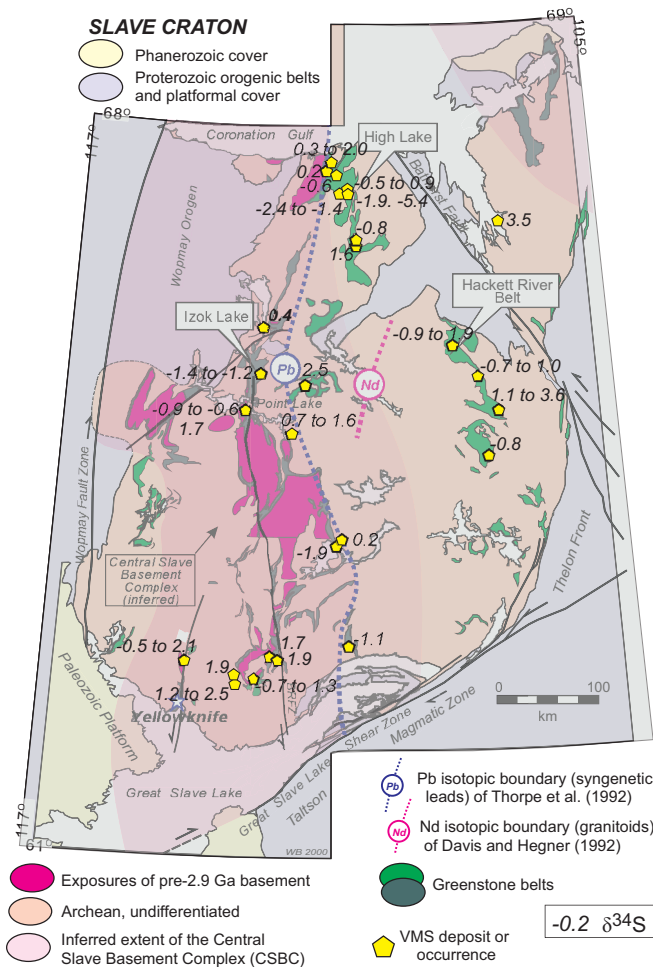


Figure 10. Map showing the distribution and, in some cases, range, of $\delta^{34}\text{S}$ values for pure and mixed sulphide samples from volcanogenic massive sulphide deposits in the Slave Craton. Although both mass-dependent fractionation (MDF) and mass-independent fractionation (MIF) processes played an important role in determining the $\delta^{34}\text{S}$ values plotted in this figure, a correlation between $\delta^{34}\text{S}$ and the age of crust, Pb isotope (Thorpe et al., 1992), and Nd isotope (Davis and Hegner, 1992) lines is not apparent. See Figure 1 for additional legend information.

Figure 12, the “bimodal rift environment” of Bleeker and Hall (2007) corresponds with the ‘bimodal-mafic’ VMS deposit type of Franklin et al. (2005a,b), and the “arc-like” setting to their ‘bimodal-felsic’ VMS deposit type. The Gondor deposit (Bubar and Heslop, 1985) is the single exception to this general association among the deposits represented in Figure 12. The deposit is hosted by felsic pyroclastic and volcanoclastic rocks, and is situated ~1 km above a presumed heat-providing, felsic subvolcanic porphyry intrusion (Bubar and Heslop, 1985; Fig. 3). Bubar and Heslop (1985) suggested that a felsic caldera developed in response to extension and subsidence in the underlying mafic (oceanic) crust. The thickness of this mafic crust evidently prompted the deposit-type classification of bimodal-mafic (Franklin et al., 2005a,b).

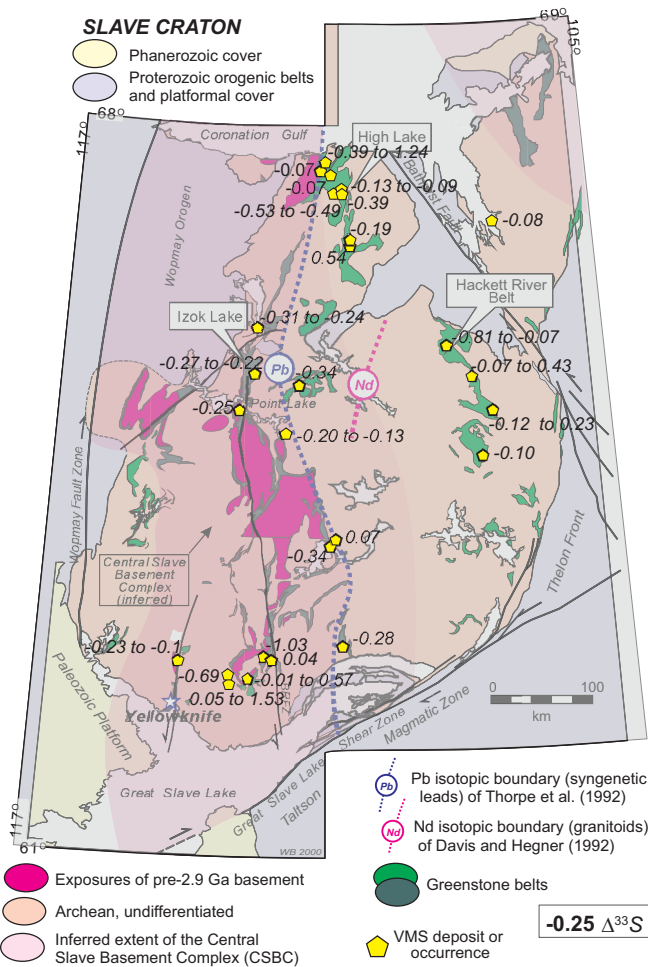


Figure 11. Map showing the distribution and (where applicable) range of $\Delta^{33}\text{S}$ for pure and mixed sulphide samples from VMS deposits in the Slave Craton. Correlations between $\Delta^{33}\text{S}$ and older crust, Pb isotope (Thorpe et al., 1992), and Nd isotope (Davis and Hegner, 1992) lines are not apparent. However, variations in $\Delta^{33}\text{S}$ may correlate with tectonic environment (see Fig. 12). See Figure 1 for additional legend information.

Although the multiple sulphur isotope systematics of VMS deposits constituted our principal focus, we sought correlations with other significant characteristics of the deposits; silver was selected. In Figure 12, the contrasting silver grades of the deposits appear to broadly correspond to the classifications of “bimodal rift” (or bimodal-mafic) and “arc-like” (or bimodal felsic). VMS deposits from “arc-like” settings have grades of >100 g/t Ag; deposits include Hackett River (160–231 g/t), Musk (343 g/t), Sunrise Lake (172 g/t), and Turnback Lake (XL; 102 g/t), Indian Mountain (116.6 g/t), and Yava Lake (102 g/t) (Franklin et al., 2005b; Campbell, 2007). The Gondor and Izok Lake deposits are exceptions, with silver grades of 46 and 73 g/t, respectively (Franklin et al., 2005b; MMG Ltd., 2013). In contrast to most deposits in the “arc-like”

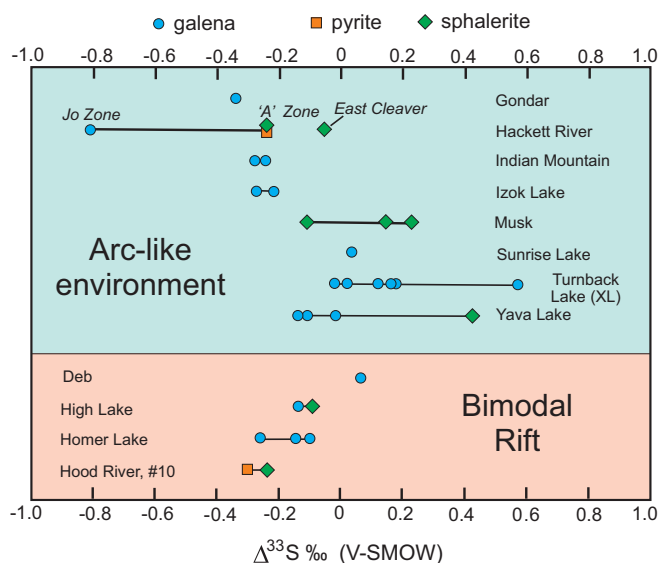


Figure 12. Comparison of $\Delta^{33}\text{S}$ values from selected VMS deposits, grouped according to their interpreted tectonic environment, as classified by Bleeker and Hall (2007). Deposits formed in arc-like environments (see sample location and index in Fig. 1) may be associated with a larger range of $\Delta^{33}\text{S}$ than observed for deposits formed in a bimodal-rift environment where mantle-derived sulphur appears to dominate. The large negative value of $\Delta^{33}\text{S}$ for the Jo zone at Hackett River is interpreted to be due to greater contributions of sulphur from reduced seawater sulphate.

environment, deposits in the “bimodal rift” category all have silver grades of <100 g/t. These include Deb (21.9 g/t), High Lake (75 g/t), Homer Lake (69.3 g/t), and Hood #10 (34 g/t) (Franklin et al., 2005b; TerraX, 2015). Thus, the two general tectonic settings distinguished in Figure 12 typically also correspond to contrasts in silver grades and magmatic association (bimodal-mafic versus bimodal-felsic), which may suggest a connection with magma genesis (e.g. juvenile character) and evolution (e.g. fractional crystallization versus crustal melt). Nevertheless, the tectonic environments in which these VMS deposits formed (and associated host rock/magma compositions), also have influenced the sulphur isotope systematics of the deposits.

Our limited database shows that VMS deposits in the bimodal rift (bimodal-mafic) environment display a restricted range of $\Delta^{33}\text{S}$, primarily -0.2 to 0‰ (Fig. 12). In contrast, VMS deposits in “arc-like” tectonic environments display a broader range of $\Delta^{33}\text{S}$ values, spanning -0.8 to 0.6‰ . Although our study is reconnaissance in nature, and additional information regarding the tectonic settings of all of the deposits analyzed is needed, the relationship in Figure 12 suggests that there may be differences in factors influencing the involvement of atmosphere-derived sulphur in these two tectonic environments. For example, VMS deposits formed in bimodal rift/bimodal-mafic rift

environments may represent deeper water settings associated with high-temperature mafic magmatism. The values of $\Delta^{33}\text{S}$ plotted in Figure 12 suggest minimal sulphur contributions from other than mantle sources, whether directly (i.e. magmatic degassing) or indirectly (e.g. leached from mantle rocks during alteration processes). However, VMS deposits in arc-like settings appear to have a larger range of $\Delta^{33}\text{S}$, including both positive and negative values, indicating the incorporation of some atmosphere-derived sulphur. These environments could include slightly younger, and more evolved magmatism in the arc-like setting (see Bleeker and Hall, 2007), increased diversity of (more-evolved) host rocks, and shallow-water (perhaps even subaerial) volcanism and settings. The arc-like (bimodal-felsic) environment evidently facilitated the increased incorporation of MIF sulphur, potentially involving additional surface sources as well as crustal (via hydrothermal recycling; see Fig. 3). Note, however, that the correspondence of higher Ag contents with greater contributions of MIF sulphur is only apparent (and due to geological association) and not causative. Nevertheless, the recognition of VMS mineralization with relatively greater amounts of atmospheric sulphur through multi-sulphur isotope analysis may prove useful in paleotectonic setting and volcanic environment determination and terrain assessment in greenfields VMS exploration.

IMPLICATIONS FOR EXPLORATION

The potential correlation between environment and factors promoting precious metal enrichment (e.g. redox conditions) suggests that further study and application of multi-sulphur isotope analysis will broaden our understanding of important aspects of deposit genesis. Although detection (and quantification) of MIF sulphur is not likely to constitute a camp-scale “vector”, it may assist in comparison and selection of potential precious metal-rich VMS environments for further exploration.

SUMMARY AND CONCLUSIONS

Volcanogenic massive sulphide deposits throughout the Slave Province contain variable contributions of atmosphere-derived (i.e. surface-processed) sulphur based on the values and ranges of $\Delta^{33}\text{S}$ determined in this study. Moreover, the contrast in two principal tectonic environments hosting VMS deposits appears to be also reflected by both the silver grades of the deposits and their sulphur isotope systematics, particularly the contributions of atmospheric sulphur. Assessment of paleotectonic settings and volcanic environments and mineralization processes can benefit from multi-sulphur isotope studies.

FUTURE WORK

Comparison with multi-sulphur isotope studies elsewhere, a broader assessment of metal and Pb isotope ratios, and analysis of the tectonic environments of each deposit remain as goals for this study. The unique significance of $\Delta^{33}\text{S}$ as a definitive tracer of Archean atmospheric sulphur demands a detailed study of one or several selected deposits in the Slave Province. Such a study would provide a better understanding of (1) the timing of acquisition of $\Delta^{33}\text{S}$ anomalies, (2) a better assessment of the balance of magmatic versus environmental sulphur sources, and (3) improved assessment of the apparent association of MIF with tectonic environment. The study of Sharman et al. (in press) in Noranda, Quebec suggests that small shifts in $\Delta^{33}\text{S}$ are controlled by the local geological environment and may be associated with the precious metal (gold) contents. The use of $\Delta^{33}\text{S}$ as a potential tracer in Archean VMS studies can also be applied to younger VMS deposits in comparable settings, but requires exceptionally high-precision techniques (Ono et al., 2007). The unique tracing capabilities due to MIF sulphur in the Archean makes detailed studies of Archean VMS deposits by the techniques employed in this study more tractable. Constraints and processes determined by studies of ancient deposits would apply to younger examples.

ACKNOWLEDGEMENTS

This study could not have been completed without the legacy collections of Ralph Thorpe, which were carefully archived by the Geological Survey of Canada. Anne Theriault kindly facilitated their access. Andre Pellerin and Thi Hao Bu are thanked for assisting with various technical aspects of this study, especially in testing of the gas chromatograph-based sample purification line added to MILES. We thank J. Jamieson for a review of this contribution.

REFERENCES

- Bleeker, W. and Hall, B., 2007. The Slave Craton: geological and metamorphic evolution, *In: Mineral Deposits of Canada: A Synthesis of Major Deposit Types, District Metallogeny, the Evolution of Geological Provinces, and Exploration Methods*, (ed.) W.D. Goodfellow; Geological Association of Canada, Mineral Deposits Division, Special Publication 5, p. 849–879.
- Bubar, D.S. and Heslop, J.B., 1985. Geology of the Gondor volcanogenic massive sulphide deposit, Slave Province, NWT; Canadian Institute of Mining and Metallurgy Bulletin, v. 78, p. 52–60.
- Campbell, C. (ed.), 2007. A guide to mineral deposits of the Northwest Territories; Department of Industry, Tourism and Investment, 206 p.
- Cawood P.A., Kröner A., and Pisarevsky S., 2006. Precambrian plate tectonics: Criteria and evidence; *GSA Today*, v. 16, p. 4–11.
- Claypool, G.E., Holser, W.T., Kaplan, I.R., Sakai, H., and Zak, I., 1980. The age curve of sulphur and oxygen isotopes in marine sulfate and their mutual interpretation; *Chemical Geology*, v. 28, p. 199–260.
- Davis, W.J. and Hegner, E., 1992. Neodymium isotopic evidence for the tectonic assembly of late Archean crust in the Slave Province, Northwest Canada; *Contributions to Mineralogy and Petrology*, v. 111, p. 493–504.
- Farquhar, J., Bao, H., and Thiemens, M., 2000. Atmospheric influence of Earth's earliest sulfur cycle; *Science*, v. 289, p. 756–758.
- Farquhar, J., Savarino, J., Airieau, S., and Thiemens, M., 2001. Observation of wavelength-sensitive mass-independent sulfur isotope effects during SO_2 photolysis: Implications for the early atmosphere; *Journal of Geophysical Research*, v. 106, p. 32829–32839.
- Farquhar, J. and Wing, B.A., 2003. Multiple sulfur isotopes and the evolution of the atmosphere; *Earth and Planetary Science Letters*, v. 6707, p. 1–13.
- Farquhar, J., Wu, N., Canfield, E.D., and Oduro, H., 2010. Connections between sulfur cycle evolution, sulfur isotopes, sediments, and base metal sulfide deposits; *Economic Geology*, v. 105, p. 509–533.
- Franklin, J.M., Gibson, H.L., Jonasson, I.R., and Galley, A.G., 2005a. Volcanogenic massive sulfide deposits, *In: Economic Geology 100th Anniversary Volume*, (ed.) J.W. Hedenquist, J.F.H. Thompson, R.J. Goldfarb, and J.P. Richards; Society of Economic Geologists, Littleton, Colorado, p. 523–560.
- Franklin, J.M., Gibson, H.L., Jonasson, I.R., and Galley, A.G., 2005b. Volcanogenic massive sulfide deposits, *In: Economic Geology 100th Anniversary Volume*, (ed.) J.W. Hedenquist, J.F.H. Thompson, R.J. Goldfarb, and J.P. Richards; Society of Economic Geologists, Littleton, Colorado, p. 1–45.
- Holland, H.D., 2006. The oxygenation of the atmosphere and oceans; *Philosophical Transactions of the Royal Society B: Biological Sciences*, v. 361, p. 903–915.
- Huston, D.L., 1999. Stable isotopes and their significance for understanding the genesis of volcanic-hosted massive sulfide deposits, *In: Volcanic-Associated Massive Sulfide Deposits: Processes and Examples in Modern and Ancient Settings*, (ed.) C.T. Barrie and M.D. Hannington; *Reviews in Economic Geology*, v. 8, p. 157–179.
- Jamieson, J.W., Wing, B.A., Farquhar, J., and Hannington, M.D., 2013. Neoproterozoic seawater sulphate concentrations from sulphur isotopes in massive sulphide ore; *Nature Geoscience*, v. 6, p. 61–64.
- MMG Ltd., 2013. Annual Report, 164 p. <http://www.mmg.com/en/Investors-and-Media/Reports-and-Presentations/Annual-Reports.aspx>
- Ohmoto, H., Mizukami, M., Drummond, S.E., Eldridge, C.S., Pisutha-Arnond, V., and Lenaugh, T.C., 1983. Chemical processes in Kuroko formation, *In: The Kuroko and Related Volcanogenic Massive Sulfide Deposits*, (ed.) H. Ohmoto and B.J. Skinner; *Economic Geology*, Monograph 5, p. 570–604.
- Ohmoto, H., Watanabe, Y., Ikema, H., Poulson, S.R., and Taylor, B.E., 2006. Sulphur isotope evidence for an oxic Archean atmosphere; *Nature*, v. 442, p. 908–911.
- Ono, S., Shanks, W.C., III, Rouxel, O.J., and Rumble, D., 2007. $\delta^{33}\text{S}$ constraints on the seawater sulfate contribution in modern seafloor hydrothermal vent sulfides; *Geochimica et Cosmochimica Acta*, v. 71, p. 1170–1182.
- Paris, G., Adkins, J.F., Sessions, A.L., Webb, S.M., and Fischer, W.W., 2014. Neoproterozoic carbonate-associated sulfate records positive anomalies; *Science*, v. 346, p. 739–741.
- Planavsky, N.J., Asael, D., Hofmann, A., Reinhard, C.T., Lalonde, S.V., Knudsen, A., Wang, X., Ossa, F.O., Pecoits, E., Smith, A.B.J., Beukes, N.J., Bekker, A., Johnson, T. M., Konhauser, K.O., Lyons, T.W., and Rouxel, O.J., 2014. Evidence for oxy-

- genic photosynthesis half a billion years before the Great Oxidation Event; *Nature Geoscience* v. 7, p. 283–286.
- Pufahl, P.K. and Hiatt, E.E., 2012. Oxygenation of the Earth's atmosphere-ocean system: A review of physical and chemical sedimentological responses; *Marine and Petroleum Geology*, v. 32, p. 1–20.
- Sasaki, A., 1970. Seawater sulfate as a possible determinant for sulfur isotopic compositions of some strata-bound sulfide ores; *Geochemical Journal*, v. 4, p. 41–51.
- Sangster, D.F., 1968. Relative sulphur isotope abundances of ancient seas and strata-bound sulphide deposits, *In: Proceedings; Geological Association of Canada*, v. 19, p. 79–91.
- Sharman, E.R., Taylor, B.E., Minarik, W.G., Dubé, B., and Wing, B.W., in press. Sulfur isotope and trace element data from ore sulfides in the Noranda district (Abitibi, Canada): implications for volcanogenic massive sulfide deposit genesis; *Mineralium Deposita*.
- Taylor, B.E., 2004. Fluorination methods in stable isotope analysis, Chapter 20 *In: Handbook of Stable Isotope Analytical Techniques*, Volume 1, (ed.) P.A. de Groot; Elsevier Science, p. 400–472.
- Terra X, 2015. prospectus, available at <http://www.terraxminerals.com/s/Home.asp>
- Thorpe, R.I., 2008. Release of lead isotope data in 4 databases: Canadian, Western Superior, foreign, and whole rock and feldspar; *Geological Survey of Canada*, Open File 5664, 42 p.
- Thorpe, R.I., Cumming, G.L., and Mortensen, J.K., 1992. A significant Pb isotope boundary in the Slave Province and its probable relation to ancient basement in the western Slave Province; *Geological Survey of Canada*, Open File Report 2484, p. 179–184.
- Zhelezinskaia, I., Kaufman, A.J., Farquhar, J., and Cliff, J., 2014. Large sulfur isotope fractionations associated with Neoproterozoic microbial sulfate reduction; *Science*, v. 346, p. 742–744.